A Novel Prevailing Torque Threaded Fastener and its Analysis

B S C Ranjan[1], Vikranth H N[1], Ashitava Ghosal[2#]

[1]Centre for Product Design and Manufacturing, [2#]Dept. of Mechanical Engineering
Indian Institute of Science, Bengaluru-560012, India
[#]corresponding author: asitava@mecheng.iisc.ernet.in

ABSTRACT

We present a novel concept of a threaded fastener that is resistant to loosening under vibration. The anti-loosening feature does not use any additional element and is based on modifying the geometry of the thread in the bolt. In a normal nut and bolt combination, the axial motion of the nut or bolt is *linearly* related to the rotation by a constant pitch. In the proposed concept, the axial motion in the bolt is chosen to be a *cubic* function of the rotation, while for the nut, the axial motion remains linearly related to the rotation. This mismatch results in interference during the tightening process and additional torque required to overcome this interference gives rise to the enhanced anti-loosening property. In addition, the cubic curve is designed to ensure that the mismatch results in stresses and deformation in the *elastic* region of the chosen material. This ensures that the nut can be removed and reused while maintaining a repeatable anti-loosening property in the threaded fastener. A finite element analysis demonstrates the feasibility of this concept.

Keywords: Threaded fasteners, Loosening, Cubic curve, Interference, Prevailing torque

1 Introduction

Threaded fasteners have rendered themselves indispensable in the assembly of mechanical systems and structures due to their ease of disassembly and their relatively low cost. The outstanding feature of threaded fasteners is that, despite their design simplicity, they provide a high clamping force. A comprehensive literature study has been carried out in [1] describing the history as well as evolution of threaded fasteners. However, the threaded fasteners have an inherent limitation that they loosen under dynamic external loads such as impact, vibration, and thermal loadings. This necessitates a high frequency of routine maintenance of the components, the absence of which may result in fatal accidents.

Research on loosening of threaded fasteners due to vibration spans nearly six decades. The reader is referred to Hess [2] and Bickford [3] for a comprehensive review of the literature. Early works [4–6] focused on loosening due to dynamic loads acting along the fastener axis (axial loading). However, experimental studies in the late 1960s by Junker [7] demonstrated that loosening is more severe when the joint is subjected to dynamic loads perpendicular to the thread axis (shear loading). Loosening under shear loading was attributed to reduction of circumferential holding friction as a result of slip at the fastener surfaces caused by the applied shear load. There have been numerous attempts [8–15] to model the loosening phenomenon; however, all have had limited success in adequately predicting loosening. It was recently shown in [16] that a fastener could turn loose under dynamic shear loading as a result of accumulation of localized slip in the form of strain at the fastener contact surfaces. Pai and Hess [17] performed a three-dimensional finite element calculation to understand the contact states of bolt head and thread surfaces for loosening. A review [18] of research on vibration and shock-induced loosening of threaded fasteners highlights one key aspect, i.e., the primary mechanism of self-loosening is relative slip within the threads and fastener nut or head interfaces. The slip is caused by forces and moments that manifest themselves in joints through bending, pressure fluctuations, shocks, impacts, thermal expansion, and axial force fluctuations [19].

In order to prevent loosening and its consequent problems, various threaded fastener designs have been patented as well as published in reputed journals [20-33]. These include modified or distorted threads and nut body such as an all-metal prevailing-torque locknut having two substantially equally spaced indentations in its top end face [22], an internally threaded nut body and having a portion of the exterior surface of the nut body provided with an irregular configuration [23], thread form truncated to partial depth with thin wall [24], steeper flank angles and truncated roots [30] and a thin walled tubular threaded metal insert [32]. A traditional way to prevent loosening is to use washers, inserts and locking units such as in locking units with asymmetric tines and grooved bolt [28], wave thread portion of the male thread and a conical spring washer [29] and threaded metal insert [32]. Other approaches use nut with split portions at one end [26] or nut with slots at one end [27], metallurgically bonded metal patch [25], resin deposits [31] and use of nylon or thermoplastic patches on the unmodified thread surfaces [33]. Several investigations have been carried out to assess the performance of these anti-loosening fasteners under vibration [1, 34]. However, it has been observed that these anti-loosening fasteners invariably suffer from one or more of the following limitations – use of additional components such as pins, washers, lock-nuts; deterioration of prevailing torque due to wear; plastic deformation of threads; high cost; non-reusability; feasibility issues in terms of manufacturing and adaptability [1, 20, 34 -36]. As a result, search for a novel design for anti-loosening fastener mechanism with optimal performance still continues.

In this paper, we propose a novel threaded fastener design with enhanced resistance to loosening and without sacrificing any of the advantageous features of conventional screw fasteners. The proposed design uses no additional components, provides predictable and repeatable prevailing torque and is reusable. The key features of the proposed concept are a) the use of a *cubic function* relating the axial and rotational motion in the bolt (instead of a constant pitch) and a *constant pitch in the nut*, b) *resulting interference* between the nut and bolt threads due to the mismatch in geometry, and c) a carefully chosen interference value such that the deformation and stresses in the nut and bolt, due to the interference, is always in the *elastic region of the material*. The cubic function results in a non-helical curve of the thread in the nut or the bolt, and when a non-helical curve is *forced* to mate with a regular helical curve, an interference results. To overcome this interference, additional torque is required during tightening, and this additional torque must be available during the loosening process, resulting in enhanced anti-loosening property. It is ensured that the additional torque does not lead to plastic deformation and hence the fastener can be removed and reused with a predictable and repeatable anti-loosening property. It can be seen that no additional material such as a pin, lock-nut, washer, glue or plastic, is used to achieve this enhanced anti-loosening property.

This paper is organized as follows: In section 2, the details and theoretical background of the proposed concepts are outlined. Section 3 provides a brief description of the solid modeling, and finite element analyses carried out. Section 4 outlines the calculation of additional torque required and Section 5 discusses the results, illustrating the feasibility of the concept.

2 Proposed Concept

In a regular nut and bolt combination, as the nut is rotated and the bolt is held fixed, the nut advances along the axis of the bolt by a fixed distance known as the pitch of the thread. A point at the contact between the nut and the bolt with coordinates (*x, y, z*) follows a helix, whose equation is given as

$$x(\theta)=R\cos(\theta);\ y(\theta)=R\sin(\theta);\ z(\theta)=\frac{P\theta}{2\pi} \tag{1}$$

where P is the pitch of the thread, R is the radius of the nut or bolt, and the angle of rotation θ lies between [0, 2π]. It may be noted that P is standardized for a given diameter of the nut or bolt. For example, for the ISO Metric size 10 (M10 or R = 5mm), the pitch P is 1.5 mm for *coarse* threads and 1.25 mm for *fine* threads. From the above equations, it follows that the advancement of the thread in the axial or Z-direction is directly proportional to the angle of rotation θ, i.e., z varies *linearly* with θ.

In the proposed concept, the `linear helical curve' is replaced by a `cubic helical curve'. The equations governing the thread curve are now given by

$$x(\theta')=R\cos(\theta');\ y(\theta')=R\sin(\theta');\ z(\theta')=a_0+a_1\theta'+a_2\theta'^2+a_3\theta'^3 \tag{2}$$

where $\theta'=\left(\frac{\theta}{2\pi}\right)$ and varies in the range [0, 1]. It may be noted that $z(\theta')$ must be multiplied by 2π to obtain $z(\theta)$. Two of the coefficients of the cubic curve can be determined by using the fact that at $\theta=0$, $z=0$ and at $\theta=2\pi$, $z=P$. Hence, we can write using two new symbols, r and s, as

$$a_0=0;\ a_1=r;\ a_2=3P-2r-s;\ a_3=r+s-2P \tag{3}$$

where $P=1.5$ mm at $\theta=2\pi$ for *coarse* M10 or $P=1.25$mm for *fine* M10 thread. In the above equations, the variables r and s determine the slope of the cubic curve at $\theta=0$ and $\theta=2\pi$, respectively[1]. As can be observed from equations (1) and (2), while the functions for the x and y coordinates of both curves remain the same, the z coordinate, which is along the axial direction (profile advancement along the length of the thread), can be varied by changing the values of r and s. It may be also be noted that for a full rotation of $\theta=2\pi$, *the axial advancement is still the pitch of the thread*. The idea of using a cubic curve is to make the curve at the beginning and end more flat as shown in Figure 1.

[1] We have used r and s as equal to ensure slope continuity between two successive cubic helix profiles along the nut or bolt.

As the cubic curve is made more flat at the beginning and at the end, the maximum deviation between the straight line and the cubic curve, denoted by δ and shown in figure 1, will be larger.

The distance, δ, between $z(\theta')$ of the cubic curve and $z(\theta')$ of the straight line is given by

$$\delta(\theta') = [a_0 + a_1\theta' + a_2\theta'^2 + a_3\theta'^3] - [P\theta'] \tag{4}$$

where the coefficients of the cubic curve are given in equation (3) and they are functions of *r* and *s*. The extreme value of $\delta(\theta')$ can be obtained by setting the partial derivative of $\delta(\theta')$ with respect to θ' to zero. We get

$$a_1 + 2a_2\theta' + 3a_3\theta'^2 - P = 0 \tag{5}$$

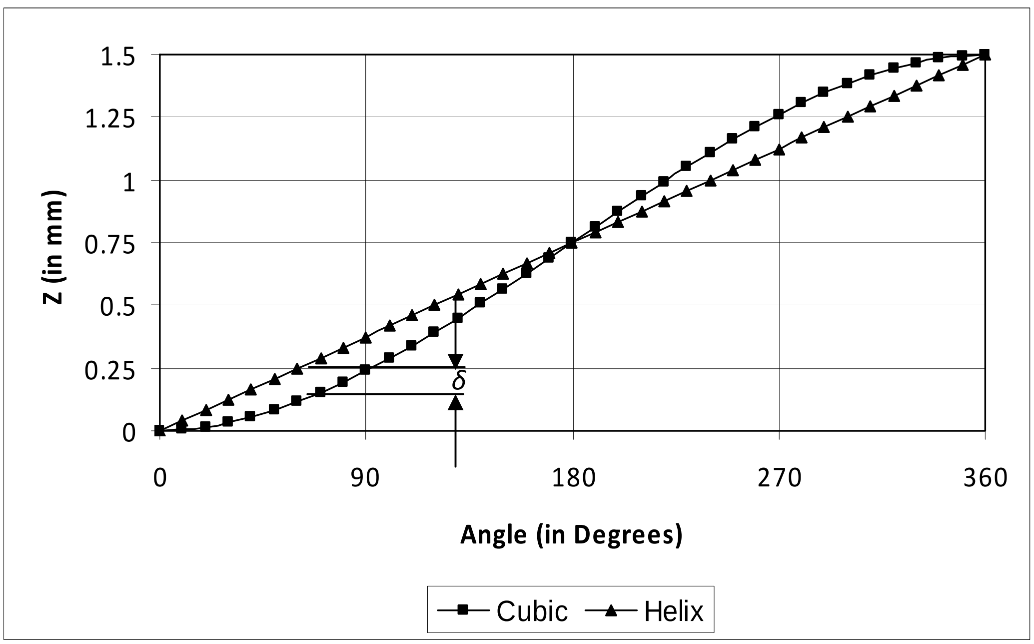

Figure 1: Comparison of the *z* coordinate in cubic and linear helical curve for M10 (*r* = 0.01, *s* = 0.01)

Therefore, the maximum and minimum δ happens at

$$\theta' = \frac{-2a_2 \pm \sqrt{4a_2^{\,2} - 12a_3(a_1 - P)}}{6a_3} \tag{6}$$

Substituting the value of θ' from (6) in (4) results in following:

$$\delta(\theta') = \left[\begin{array}{c} a_0 + \left(\dfrac{(a_1 - P)(-2a_2 \pm (\sqrt{4a_2^{\,2} - 12a_3(a_1 - P)}}{6a_3}\right) + \\ a_2\left(\dfrac{(-2a_2 \pm (\sqrt{4a_2^{\,2} - 12a_3(a_1 - P)}}{6a_3}\right)^2 + a_3\left(\dfrac{(-2a_2 \pm (\sqrt{4a_2^{\,2} - 12a_3(a_1 - P)}}{6a_3}\right)^3 \end{array}\right] \tag{7}$$

It may be noted that the maximum δ occurs at $\theta = 76.07^\circ$ for an M10 coarse thread, and Table 1 presents the theoretical maximum interference, δ, for various values of *r* and *s*. The range of the values of *r* and *s* is chosen such that their values give rise to an interference that is *not smaller* than the typical manufacturing tolerance of about 30 microns (for M10). At the same time, the interference should not result in plastic deformation that would make the nut/bolt non reusable and the prevailing torque value unpredictable. In section 4, we present stresses, obtained from a finite element analysis, due to the interference of a cubic bolt and regular nut with various *r* and *s* values.

	r	***s***	**Interference (in mm)**
1	0.236	0.236	0.0017
2	0.235	0.235	0.0023
3	0.23	0.23	0.0053
4	0.21	0.21	0.0174
5	0.19	0.19	0.0295
6	0.17	0.17	0.0416
7	0.15	0.15	0.0536
8	0.13	0.13	0.0657
9	0.11	0.11	0.0778
10	0.09	0.09	0.0899
11	0.07	0.07	0.1020
12	0.05	0.05	0.1141

Table 1: Theoretical interference at different values of *r* and *s*, at $\theta = 76.07^\circ$

The difference between the linear and cubic function can also be visualized by the lead angle as shown in Figure 2. The lead angle for the regular helical curve is constant, whereas for the cubic curve, the lead angle at the beginning and at the end is smaller. The lead angle for cubic curve is higher at the middle as compared to the helix profiles, and the slope of the cubic curve is varying at every point. The cubic variation of *z* gives rise to an instantaneously variable pitch.

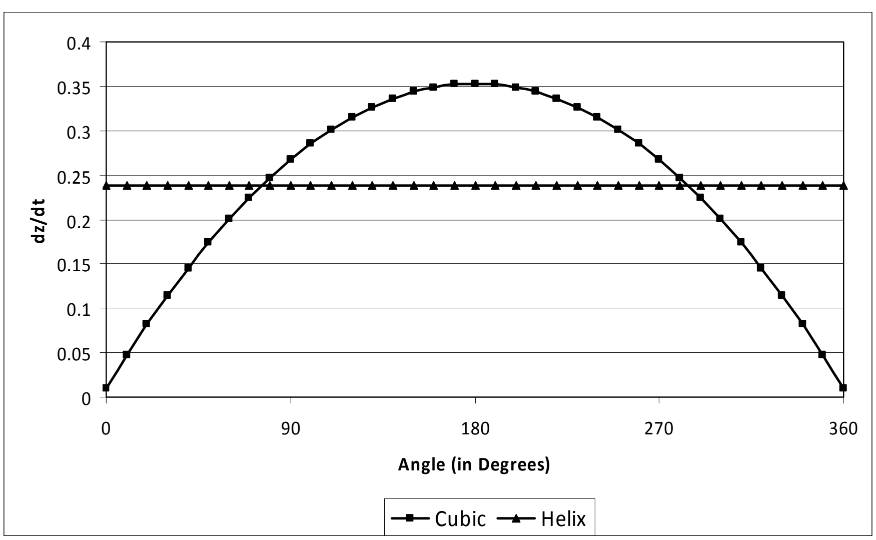

Figure 2: Variation of lead angle for regular helix and cubic curves

As mentioned above and from equation (2) and (3), by varying *r* and *s,* different cubic curves can be obtained with varying deviation from the helix. In addition to Figure 1, some more examples are shown in Figure 3 to illustrate this observation. Figure 3 also illustrates, graphically, the effect of the varying the values of the variables of *r* and *s*.

As discussed earlier, if a *regular* helical nut is forced to mate with a *cubic* bolt, there will be interference at some locations. The maximum interference will be the amount δ, which is determined by *r* and *s*. In order to overcome this interference, additional torque needs to be applied to the nut or bolt, and threads of the nut and bolt will deform, leading to internal stresses being developed in the nut and bolt. During vibration, additional torque is required to overcome these internal stresses, and this gives the anti-loosening property of the nut/bolt. The key idea is to choose an appropriate *r* and *s* such that the stresses and deformation are in the elastic limit of the material and hence the deformation will go away when the nut is removed from the bolt. In addition, since the nut and bolt regain their undeformed geometries when disengaged, during reuse the deformation and stresses will be repeatable.

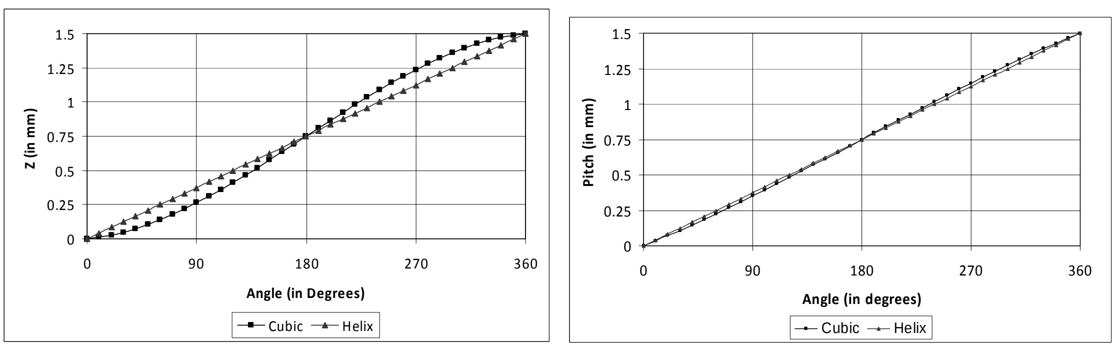

(a) r = 0.05, s = 0.05 **(b)** r = 0.20, s = 0.20

Figure 3: (a)-(b) Examples of cubic profiles with varying *r* and *s*

In the next section, we present a solid model of the 'regular nut/cubic bolt' assembly and perform *Finite Element Analyses* (FEA) to ensure that the deformations and stresses are within the elastic range. The FEA also aids in obtaining an estimate of the additional torque that is required to overcome the interference when a regular nut is *forced* to mate with a cubic bolt.

3 Solid Modeling and FEA of Proposed Cubic Thread Concept

3.1 Solid Modeling

The solid model of the M10 linear helical nut and cubic helical bolt combination is developed. The normal geometry of ISO metric screw threads for M10 is available from literature [37] and is used to model the thread profile of both the nut and the bolt. The M10 V-60° profile used is shown in Figure 4.

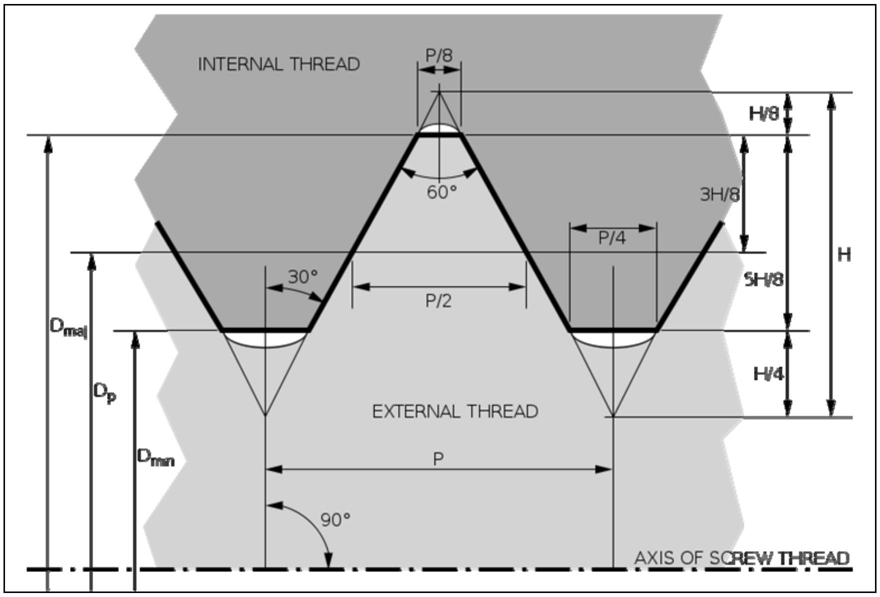

Figure 4: V-profile for ISO general-purpose metric screw threads

The bolt is modeled with *Sweep Cut* option in SolidWorks® [38] by using the above discussed profile along a path (i.e., cubic curve) whose coordinates are as per equation (2) and (3) discussed in Section 2. The regular nut is overlaid with its centerline axis co-axial with that of the 'bolt with cubic-curve' to obtain the physical interference between them, and an example is shown in Figure 5. Solid models were developed for different *r* and *s* values with the interference at $\theta = 76.07^\circ$ as shown in Table 1.

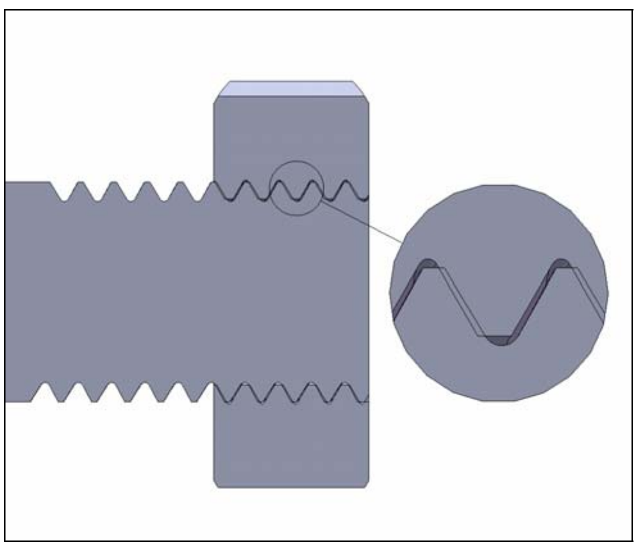

Figure 5: Sectional view at $\theta = 76.07^\circ$ corresponding to maximum interference

3.2 Finite Element Analysis

The objectives of the finite element analysis of the cubic *Z* profile bolt and linear *Z* profile nut, shown in this section are two-fold: (1) To ensure that the deformations in the nut and bolt are in the elastic region and (2) to find the approximate additional torque required to overcome the interference. The finite element analysis of the proposed concept was carried out using a commercially available software ANSYS®[39].

In this finite element analysis, the following assumptions are made: (1) the assembly of the nut and bolt is two-dimensional and axisymmetric, and (2) the material is isotropic. The procedure followed is as mentioned below:

(1) From the 3D model of the cubic-profile bolts and linear-profile nuts developed in SolidWorks®, the drawings were extracted in the plane corresponding to maximum interference (i.e., $\theta = 76.07^\circ$) for all the bolts with different *r* and *s* values. These drawings are then imported into ANSYS® for the geometry of cubic helical bolt and linear helical nut.

(2) Details of meshing are given below:

   a. **Elements**: *PLANE182* elements are used since these elements can be used for 2D modeling of solid structures as either a plane element (plane stress, plane strain or generalized plane strain) or an axisymmetric element. The element has plasticity, hyper-elasticity, stress stiffening, large deflection, and large strain capabilities. It also has mixed formulation capability for simulating deformations of nearly incompressible elasto-plastic materials and fully incompressible hyper-elastic materials.

   b. **Material Models**: A linear, isotropic material model is used since the objective of the analyses here is to restrict the deformations such that the stresses lie within the elastic limits. The material properties of steel [Young's Modulus (*E*) = 210 GPa and Poisson's ratio (*v*) = 0.30] was used for the material model.

   c. **Mesh**: The free-meshing technique for the bolt-nut model is used with the above-mentioned element type as shown in Figure 6.

(3) Details of loading are given below:

   a. The assembly of the regular helical nut and cubic bolt is imported which has a certain interference value as governed by equations (2) and (3). In the FE analysis, this interference between the two bodies is '*removed'* using an in-built contact algorithm in ANSYS® to find the stress, forces and moments in the linear nut and cubic bolt.

   b. **Contact**: The contacts between the surfaces of the linear nut and cubic bolt were built using *TARGET169* and *CONTACT171* elements.

(4) Details of boundary conditions are given below:

   a. **Pilot nodes and Boundary conditions:** Pilot nodes are created at the bottom edge of the bolt head and the outer edge of the nut using the contact manager (as shown in Figure 6). The pilot node at the bottom edge of the bolt head and the outer edge of the nut is constrained in *UX, UY* and *ROTZ* at the nodes (as shown in Figure 6).

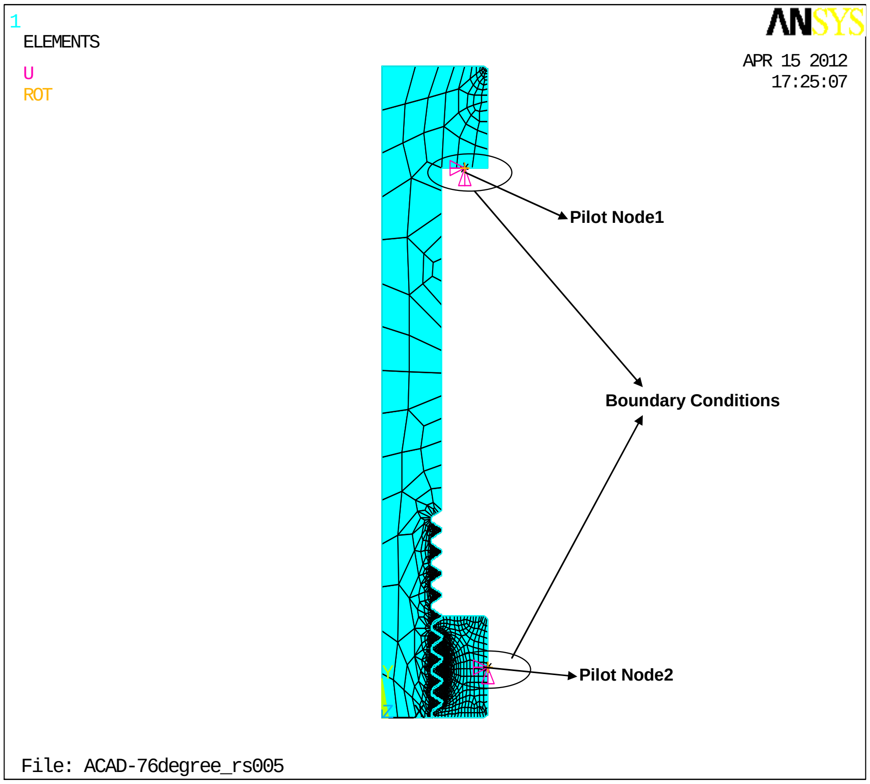

Figure 6: Meshing of model and boundary conditions used in FEA

(5) **Validation of FEA:** The geometry of the cubic bolt and regular helical nut assembly is significantly complex to formulate an analytical equation for calculating the deformations and stress values. However, the above FEA-procedure needs to be validated to assess the accuracy of the results obtained. For this, following procedure was used:

a. A 'simple interference fit between two tubes' was modeled. For this, both finite element analysis and analytical calculations to find stress are possible.

b. The 'cubic bolt and regular nut assembly' was assumed to be similar to the 'simple interference fit between two tubes' (see Figure 7) [40]. The volume of interference between the two tubes was equated to the volume of interference between nut and bolt to find the equivalent interference to be used in the 'simple interference fit between two tubes'. By using the equivalent interference in the 'simple interference fit between tubes', the assumption that it is similar to the cubic bolt and regular nut assembly becomes reasonable.

c. The pressure and stress is given by the following equation [40]:

$$\sigma = -P_c = -\frac{E\Delta}{2c^3}\frac{(c^2-a^2)(b^2-c^2)}{(b^2-a^2)} \tag{8}$$

where the dimensions a, b, c and Δ are as shown in Figure 7 below.

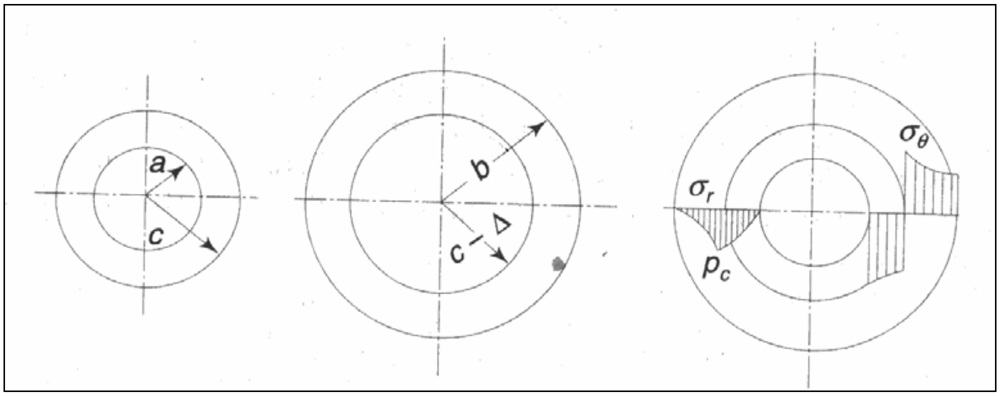

Figure 7: Stresses in composite tubes [40]

d. The following dimensions are used to calculate the contact pressure and stress: $E = 210000\text{N/mm}^2$, $a = 0\text{mm}$, $b = 9.5\text{mm}$, $c = 4.513\text{mm}$ and $\Delta = 0.012751\text{mm}$. From analytical equation (8), contact pressure and stress in the bolt are found to be $\sigma = -P_c = -229.733\text{N/mm}^2$ [negative sign indicating the compressive stress].

e. Using the plain stress FEA procedure to obtain the pressure and stress values for 'simple interference fit between tubes' using the same dimensions as used in the analytical calculations, the results are obtained. From FEA, stress in the bolt ranges from $\sigma = 215.724\text{N/mm}^2$ to $\sigma = 257.230\text{N/mm}^2$ (see the inner cylinder in Figure 8) and pressure in the bolt ranges from $P_c = 228.212\text{N/mm}^2$ to $P_c = 228.358\text{N/mm}^2$ (see Figure 8).

From the above results, it can be seen that the finite element analysis procedure used to calculate the stress matches reasonably well with the analytical results. As mentioned, earlier this validation is for two concentric cylinders with a volume of interference obtained from the regular nut and a cubic bolt.

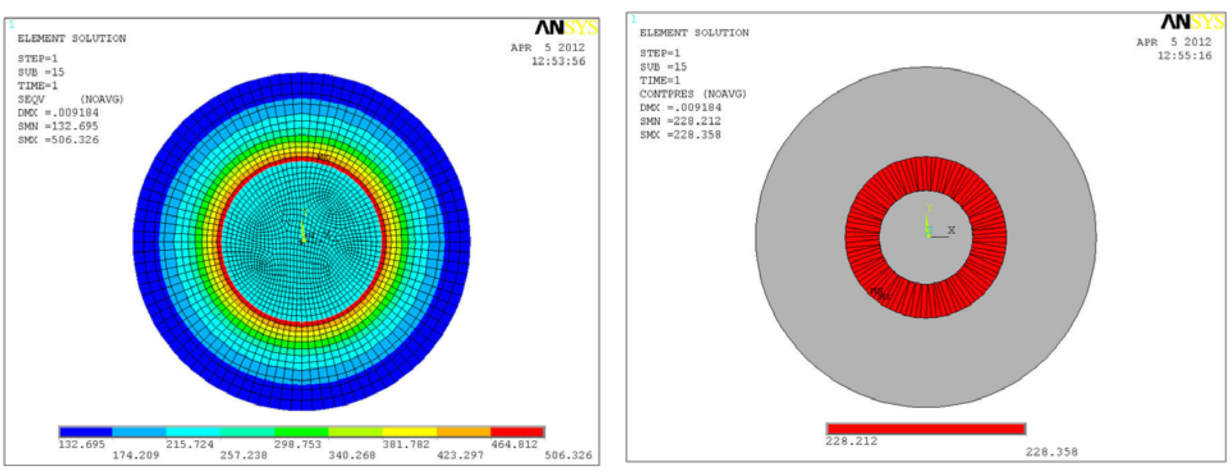

Figure 8: von-Mises stress and contact pressure of the interference fit from FEA

4 Results of FE Analyses

In this section, we present the results of the finite element analysis for the regular nut and cubic profile bolt made of steel.

4.1 Evaluation of stresses

One of the objectives of the FE analyses is to ensure that the deformations in the nut and bolt are in the elastic region. In order to determine the maximum interference possible within the elastic limit for steel material (with E = 210 Gpa and v = 0.3), the above mentioned FEA procedure is performed on models with different r and s values. From these, the stress due to the interference between the nut and bolt for different r and s values are determined. The FEA results in the form of von-Mises stresses of one representative model ($r = s = +0.17$) is shown in Figure 9 with the left figure showing the entire nut and bolt and the right figure showing the zoomed view of the nut mated with the bolt.

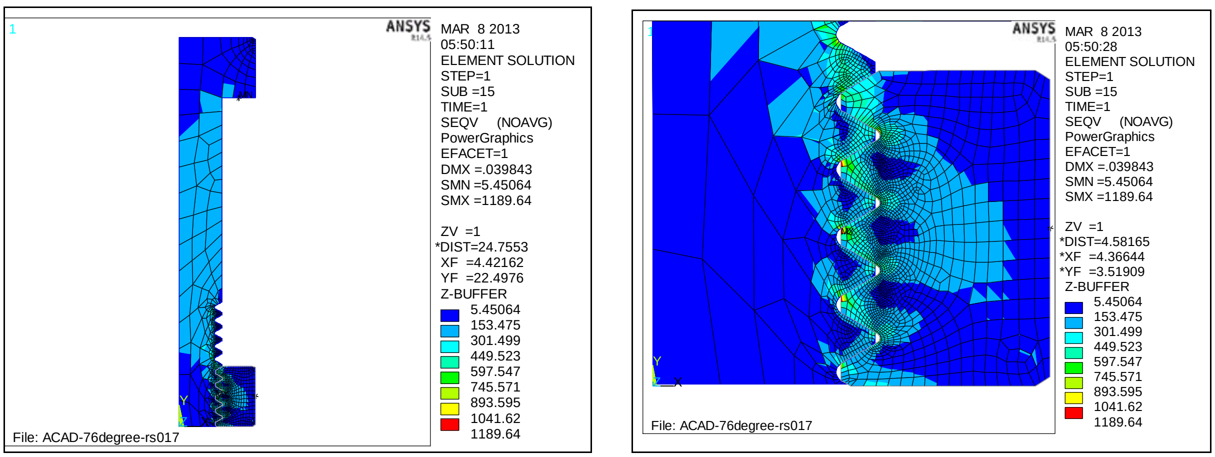

Figure 9: von-Mises stress from FEA (for $r = s = +0.17$)

As can be seen from Figure 9, the von-Mises stress at the thread tips is very high because of the stress concentration and mesh density. To normalize these high values, the von-Mises stress at the centroid of the nut thread in the sectional view (see figure 10) is chosen. These results are tabulated in Table 2. From Table 2 we can see that we have elastic deformation in steel for r and s up to 0.05. For r and s less than 0.05, the interference is more than 114 microns and the stress values go above the assumed yield value of 660 N/mm^2. For a reusable nut/bolt combination and for repeatable prevailing torque values, the r and s values must be chosen larger than 0.05.

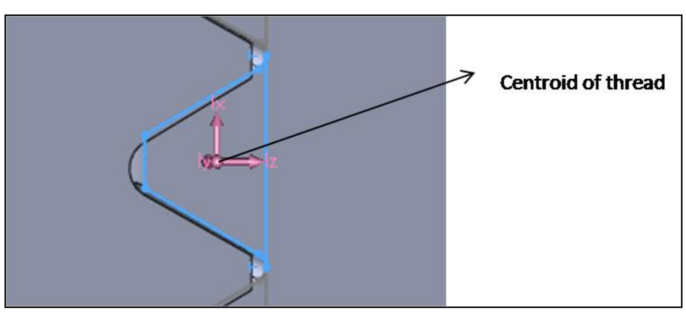

Figure 10: Centroid of the nut thread in sectional view

	r	*s*	Interference (in mm)	von-Mises Stress (N/mm^2)
1	0.236	0.236	0.0017	207.8650
2	0.235	0.235	0.0023	209.5683
3	0.23	0.23	0.0053	215.4189
4	0.21	0.21	0.0174	262.8511
5	0.19	0.19	0.0295	287.5609
6	0.17	0.17	0.0416	342.2189
7	0.15	0.15	0.0536	393.4029
8	0.13	0.13	0.0657	487.1213
9	0.11	0.11	0.0778	547.3845
10	0.09	0.09	0.0899	600.2066
11	0.07	0.07	0.1020	643.8275
12	0.05	0.05	0.1141	666.7175

Table 2: Variation of von-Mises stress for different *r* and *s* at the centroid

4.2 Torque Calculations

FEA facilitates an assessment of prevailing torque that is achieved when a regular helical nut is forced to mate with a cubic bolt. In reference [41], the following equation (9) is given to calculate the torque necessary to develop a particular preload:

$$T_i = \frac{F_y d_p(\mu + \tan\lambda\cos\alpha)}{2(\cos\alpha - \mu\tan\lambda)} \tag{9}$$

The pitch diameter d_p can be roughly approximated as the bolt diameter d

$$T_i = \frac{F_y d(\mu + \tan\lambda\cos\alpha)}{2(\cos\alpha - \mu\tan\lambda)} \tag{10}$$

Factoring out the force and bolt diameter, we get

$$T_i = K_i F_y d \tag{11}$$

$$K_i = \frac{(\mu + \tan\lambda\cos\alpha)}{2(\cos\alpha - \mu\tan\lambda)} \tag{12}$$

where, K_i is the torque co-efficient. If we assume the friction co-efficient of 0.15 and calculate the torque co-efficients K_i for all standards using the actual pitch diameters d_p rather than the approximation of the equation (9), the value of K_i varies very little over the entire range of thread sizes. Thus, the tightening torque T_i needed to obtain the desired preload force F_y in lubricated threads can be approximately obtained as

$$T_i = 0.21 F_y d \tag{13}$$

The value F_y is obtained in the post-processing phase for each set of *r* and *s* values. It can be observed in Figure 11 that the value F_y is varying linearly with the interference values. Equation (13) shows that F_y and torque T_i are linearly proportional to each other. Hence, with increase in interference values, the prevailing torque value is expected to increase. The case with highest F_y values that is still within the elastic limits is considered as acceptable for the geometry and material combination. The prevailing torque for different *r* and *s* values is calculated and shown in Table 3.

	r	***s***	**Interference (in mm)**	**Force, F_x (in N)**	**Force, F_y (in N)**	**Moment, M_z (in Nmm)**	**$T_i = 0.21F_y d$ (Nm)**
1	0.236	0.236	0.0017	7.1302	1283.8	1433.6	2.7173
2	0.235	0.235	0.0023	25.492	1512.5	1730.2	3.2795
3	0.23	0.23	0.0053	59.385	2587.6	2962.2	5.6147
4	0.21	0.21	0.0174	69.806	6895.7	7800.8	14.7861
5	0.19	0.19	0.0295	327.27	11684	13319	25.2456
6	0.17	0.17	0.0416	540.6	16070	18975	35.9663
7	0.15	0.15	0.0536	168.41	20435	23234	44.03912
8	0.13	0.13	0.0657	583.89	24318	26782	50.7642
9	0.11	0.11	0.0778	744.81	28733	32292	61.2082
10	0.09	0.09	0.0899	158.21	33099	36785	69.7245
11	0.07	0.07	0.1020	324.71	37473	40975	77.6664
12	0.05	0.05	0.1141	1208.6	42237	47413	89.8694

Table 3: Forces, moment, and torque for steel bolt due to interference

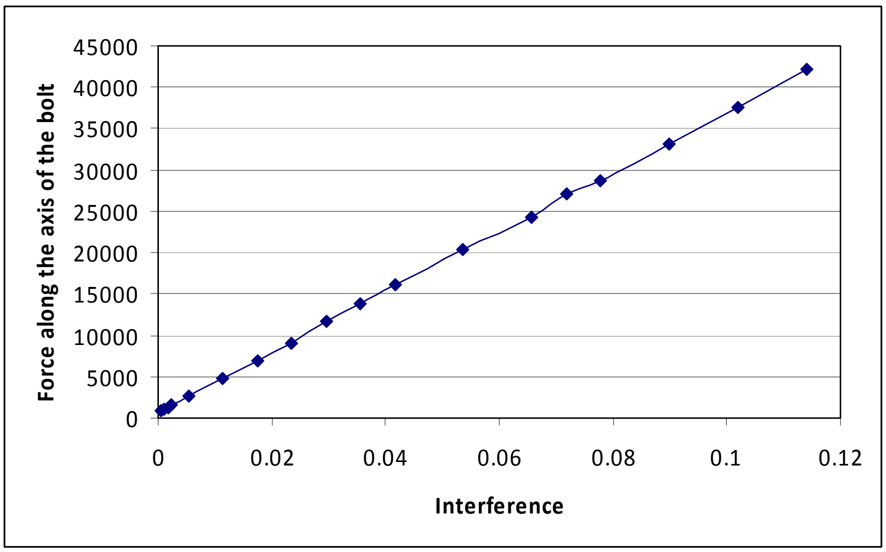

Figure 11: F_y versus interference plot (for steel)

In reference [42], the maximum permissible prevailing torque for a steel nut and bolt (property class 8) with flange with coarse thread, for the first assembly is given as 10.5 Nm. From Table 3, it can be observed that values for *r* = *s* = 0.21, the prevailing torque in a linear helical nut and cubic helical bolt combination is 14.7 Nm, i.e., 4.2 Nm larger than the maximum permissible value. This amount of torque is necessary to rotate the nut and this leads to the enhanced anti-loosening property.

4.3 Initial Experiments and Discussion

We are in the process of manufacturing a bolt with the above-mentioned features. Several things have come to our attention during the first manufacturing attempt, and we list a few of the important considerations required to experimentally validate the above conceptual design and analysis.

1) There exist standard fits and tolerances in any thread profile. This value is typically 30 microns for a M10 nut and bolt. A maximum value of the interference, which will ensure that the threads do not undergo plastic deformation, is approximately 105 microns. Hence, during manufacturing care must be taken to see that tolerances less than 50 microns are achieved in the thread profile.

2) A five-axis CNC machine is required to manufacture the cubic profile of the bolt thread. Attempts to use a 3- and 4-axis machine available in our workshop did not give satisfactory results. We manufactured two steel bolts with *r* and *s* values of 0.17 since for these values, the stresses are expected to be within the yield strength of steel (see Table 2). A scan of the manufactured bolt was performed, and the profile was overlaid on the desired profile as shown in Figure 12. Unfortunately, on inspection it was found that the precision of manufacturing was worse than ±100 microns. The stress value for an interference of 105 microns is above the yield strength of C45 steel. This meant these prototypes would certainly fail. Attempts are being made to manufacture bolts whose cubic thread profile is within 50 microns of the desired values.

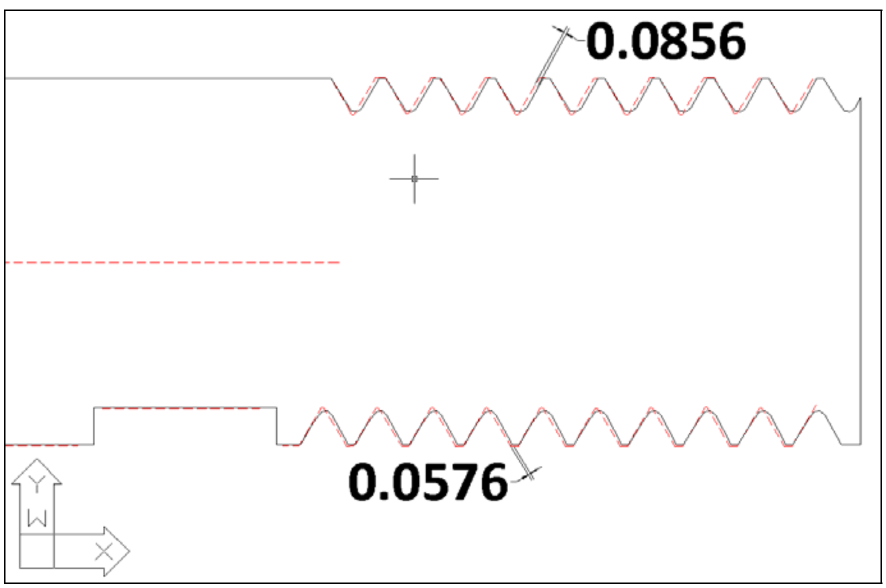

Figure 12: Comparison of the desired profile (continuous-black) and scan of manufactured bolt profile (dotted-red)

One way to avoid the problem of very tight manufacturing tolerance is to use a material that has a smaller *E* but similar yield strength, thereby allowing larger deformation before yielding. This will enable a much larger deflection than the tolerances obtained from typical manufacturing processes. It turns out that titanium alloy Ti-6Al-4V has an *E* value of 113.8 GPa and yield strength of 880 MPa which is similar to steel. *Hence, a bolt made of titanium alloy can deform much more than steel and still be in the elastic* *region.* Table 4 gives the von-Mises stress for a bolt made of titanium alloy for various *r* and *s* values obtained from finite element analyses similar to that of steel described in section 4. As it can be seen from Figure 13, the deflection can be much larger *before the material crosses its elastic limit*, and thus, the requirement of manufacturing tolerances need not be as small as in steel. We are in the process of manufacturing more precise bolts of steel and titanium so that we can validate the concept of prevailing torque due to interference experimentally.

	r	*s*	Interference (in mm)	von-Mises Stress (N/mm^2)
1	0.236	0.236	0.0017	106.65
2	0.235	0.235	0.0023	116.74
3	0.23	0.23	0.0053	125.05
4	0.21	0.21	0.0178	141.73
5	0.19	0.19	0.0295	158.69
6	0.17	0.17	0.0416	202.12
7	0.15	0.15	0.0536	216.65
8	0.13	0.13	0.0657	265.37
9	0.11	0.11	0.0778	304.95
10	0.09	0.09	0.0899	336.66
11	0.07	0.07	0.1020	356.47
12	0.05	0.05	0.114	371.14
13	0.03	0.03	0.1262	441.66
14	-0.01	-0.01	0.1504	520.43
15	-0.05	-0.05	0.1746	597.31
16	-0.09	-0.09	0.1988	651.25
17	-0.13	-0.13	0.2229	771.1

Table 4: von-Mises stress for a cubic titanium bolt for different *r* and *s*

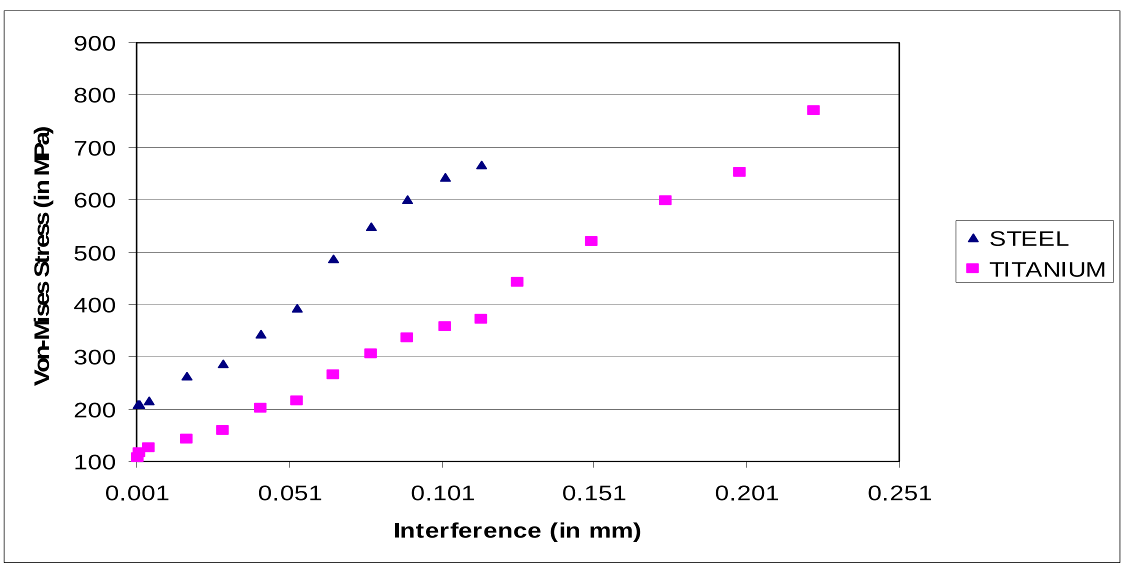

Figure 13: von-Mises stress versus interference for steel and titanium

5 Conclusions

This paper deals with a novel fastener design with the fastener expected to have significant anti-loosening features. The novelty of the design lies in the fact that no additional material is used as in traditional locking and other mechanisms. The anti-loosening feature is due to the use of a cubic advancement profile along the axis of the nut or bolt. The mating of a cubic and a regular linear (helical) profile results in interference, and the anti-loosening feature is due to the additional torque required to overcome the interference. The interference is carefully chosen such that the stresses and deformation lie in the elastic region of the material. The interference is shown to depend on two parameters which represent the slopes at the beginning and end of the cubic curve. A finite element analysis is used to ensure that the deformations in nut and bolt are in the elastic region and this analysis allows us to find the additional torque required to overcome the interference.

Acknowledgements

We like to acknowledge the Advanced Product Development and Prototyping (APDAP) at IISc Bangalore for initial data and help in early modeling and FE analysis.

References

1. Bhattacharya A, Sen A and Das S, ``An investigation on the anti-loosening characteristics of threaded fasteners under vibratory conditions'', *Mechanism and Machine Theory* **45,** pp. 1215–1225, 2010.
2. Hess D P, ``Vibration- and shock- induced loosening'', *Handbook of Bolts and Bolted Joints* (Editors Bickford J H and Nasser S), pp. 757-824, New York, Marcel Dekker, 1998.
3. Bickford J H, *An Introduction to the Design and Behavior of Bolted Joints* (third edition), Marcel Dekker, New York, 1995.
4. Goodier J N and Sweeney R J, ``Loosening by vibration of threaded fastenings'', *Mechanical Engineering*, **67**, pp. 798–802, 1945.
5. Sauer J A, Lemmon D C, and Lynn E K, ``Bolts: how to prevent their loosening'', *Machine Design,* **22**, pp. 133–139, 1950.
6. Gambrell S C, ``Why bolts loosen'', *Machine Design*, **40**, pp. 163–7, 1968.
7. Junker G H, ``New criteria for self-loosening of fasteners under vibration'', *SAE Transactions* **78**, pp. 314–35, 1969.
8. Sakai T, ``Investigations of bolt loosening mechanisms'', *Bulletin of JSME*, 21(159), pp. 1385–90, 1978.
9. Yamamoto A and Kasei S, ``A solution for self-loosening mechanism of threaded fasteners under transverse vibration'', *Bulletin Japan Society of Precision Engineering*, **18**, pp. 261–6, 1984.
10. Vinogradov O, Huang X, ``On a high frequency mechanism of self-loosening of fasteners'', *Proc. of 12th ASME Conference on Mechanical Vibration and Noise*, Montreal, Quebec, pp. 131–7, 1989.
11. Daabin A and Chow Y M, ``A theoretical model to study thread loosening'', *Mechanism and Machine Theory*, **27**, pp. 69–74, 1992.
12. Zadoks R I and Yu X, ``A preliminary study of self-loosening in bolted connections'', *ASME Nonlinear Vibrations*, DE-54:79–88, 1993.
13. Zadoks R I and Yu X, ``An investigation of the self-loosening behavior of bolts under transverse vibration'', *Journal of Sound and Vibration*, **208**, pp. 189–209, 1997.

14. Kasei S and Matsuoka H, ``Considerations of thread loosening by transverse impacts'', *ASME Pressure Vessels and Piping Division (Publication) PVP,* **367**, pp. 117–23, 1998.
15. Eccles W, Sherrington I and Arnell, R D, ``Towards an understanding of the loosening characteristics of prevailing torque nuts'', *Proc. Of the Institution of Engineers, Part C: Journal of Mechanical Engineering Science*, Vol. 224, pp. 483-495, 2010.
16. Pai N G and Hess D P, ``Experimental study of loosening of threaded fasteners due to dynamic shear loads'', *Journal of Sound and Vibration*, **253**, pp.585-602, 2002.
17. Pai N G and Hess D P, ``Three-dimensional finite element analysis of threaded fastener loosening due to dynamic shear load'', Engineering Failure Analysis, **9**, pp. 383–402, 2002.
18. Hess, D P, ``Vibration and shock–induced loosening,'' *Chapter 40, Handbook of Bolts and Bolted Joints*, Marcel Dekker Inc., New York, pp. 757–824, 1998.
19. Hess D P, ``Counter-threaded spring-actuated lock-fasteners'', *ASME Trans., Journal of Mechanical Design*, **124**, pp. 582–5, 2002.
20. Sase N, Koga S, Nishioka K and Fuji H, "An Anti- Loosening Screw Fastener Innovation and Its Evaluation", *Journal of Materials and Processing Technology*, **77,** pp.209–215, 1998.
21. Sase N, Koga S, Nishioka K and Fuji H, "Evaluation of anti-loosening nuts for screw fasteners", *Journal of Materials and Processing Technology*, **56**, pp. 321–332, 1996.
22. Frailly R A, Eaton Corporation (Cleveland, OH), *Prevailing Torque Locknut*, U.S. Pat. 3,741,266, 1973.
23. Villo J P, Standard Pressed Steel Co. (Jenkintown, PA), *Rotation Resistant Nut*, U.S. Pat. 4,005,740, 1977.
24. Holmes, H D (28576 Green Willow, Farmington Hills, MI, 48018), *Reusable Prevailing Torque Nut***,** U.S. Pat. 4,293,262, 1981.
25. Bedi, R D (6058 Wing Lake Rd., Birmingham, MI, 48010), Self locking fastener, U.S. Pat. 5,122,020, 1992.
26. Dziaba, R J (Buffalo Grove, IL), Illinois Tool Works Inc. (Glenview, IL), 1997, *Prevailing torque nut*, U.S. Pat. 5,662,443, 1997.
27. Dietlein, R W (1963 Glenbrook House Rd., Glenbrook, NV, 89413), *Fastener with relieved thread section ends*, U.S. Pat. 4,890,965, 1990.
28. Ball, L (Lloyd Harbor, NY, US), Permanent Technologies, LLC (Lloyd Harbor, NY, US), *Locking nut and bolt system with enhanced locking*, U.S. Pat. 7,374,495 B2, 2008.
29. Nebl, D R and Dohm, S R, *Fastener and assembly therewith*, U.S. Pat. 2007/0,274,805 A1, 2007.
30. Holmes, H D, *Locking fastener*, U.S. Pat. Re 31,284, 1983.
31. Duffy, R J, USM Corporation (Flemington, NJ), *Self-Locking Threaded Element*, U.S. Pat. 3,554,258, 1971.
32. Jukes J A, *Self-Locking Threaded Insert*, U.S. Pat. 3,566,947, 1971.
33. Faroni, C C and Humphrey Jr., J S, Amerace Esna Corporation (New York, NY), *Self-Locking Threaded Fastener*, U.S. Pat. 3,568,746, 1971.
34. Hess D P, Cheatham C A and Acosta C F, ``Tests and analysis of secondary locking features in threaded inserts'', *Engineering Failure Analysis*, **16**, pp. 39–57, 2009.
35. Hongo, K, "Loosening of bolt and nut fastening", *Journal of Japan Society of Mechanical Engineering*, **30,** 1964, pp. 934-939, 1964.
36. www.boltscience.com/pages/vibloose.htm, 2006.
37. Oberg, E, Jones, F D, Ryffel, H H, McCauley, C J, Heald, R M and Hussain, M I, *Machinery's Handbook 28th Edition*, Industrial Press Inc., New York, NY, 2008.
38. SolidWorks, Dassault Systems, Vélizy, France.
39. ANSYS, Ansys Inc., Pennsylvania, USA.
40. Srinath, L., *Advanced Mechanics of Solids*, McGraw Hill, 2008.
41. Norton R L, *Machine Design: An Integrated Approach*, Prentice Hall, 2011.

42. International Standard, ISO 2320:2008, Prevailing torque type steel nuts – Mechanical and performance properties.